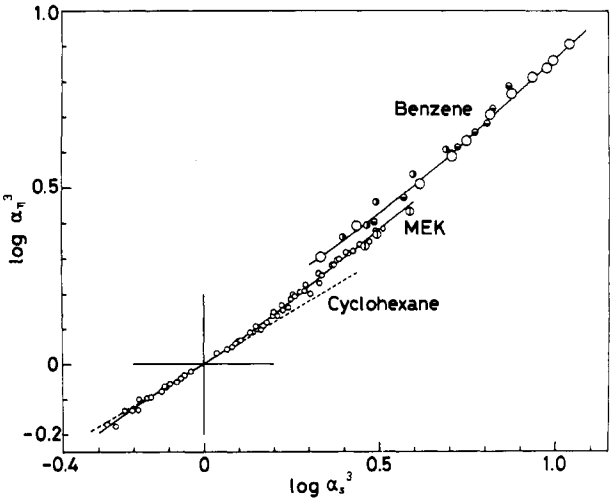

Figure 10. log-log plots of α_η^3 vs. α_s^3 for polystyrene in different solvents. Symbols are the same as in Figure 1. The dashed line is the initial tangent predicted by the perturbation theories for α_s^1 and α_η.[14]

shown above, $\langle S^2 \rangle$ of polystyrene in these three solvents obeys the two-parameter theory, this result is a clear demonstration of the breakdown of the two-parameter theory for $[\eta]$. No previous work has revealed as distinctly as seen here splitting of log α_η^3 vs. log α_s^3 plots for polystyrene in different solvents. Probably, this was due to the fact that previous measurements could not be extended to sufficiently high values of α_s^3 in MEK and cyclohexane because of the unavailability of ultrahigh molecular weight polymer samples.

Acknowledgment. We thank Dr. T. Norisuye of our laboratory for very stimulating and constructive conversations on the subject discussed in this paper.

References and Notes

(1) Yamakawa, H. "Modern Theory of Polymer Solutions"; Harper and Row: New York, 1971.
(2) Flory, P. J. *J. Chem. Phys.* **1949**, *17*, 303.
(3) Miyaki, Y.; Einaga, Y.; Fujita, H. *Macromolecules* **1978**, *11*, 1180 (Part 7 of this series).
(4) Yamamoto, A.; Fujii, M.; Tanaka, G.; Yamakawa, H. *Polym. J.* **1971**, *2*, 799.
(5) Fukuda, M.; Fukutomi, M.; Kato, Y.; Hashimoto, T. *J. Polym. Sci., Polym. Phys. Ed.* **1974**, *12*, 871.
(6) Miyaki, Y. Ph.D. Thesis, Osaka University, 1981.
(7) Matsumoto, T.; Nishioka, N.; Fujita, H. *J. Polym. Sci., Part A-2* **1972**, *10*, 23 (Part 4 of this series).
(8) Domb, C.; Barrett, A. J.; Lax, M. *J. Phys. A: Math. Gen.* **1973**, *6*, L82.
(9) Miyaki, Y.; Einaga, Y.; Fujita, H.; Fukuda, M. *Macromolecules* **1980**, *13*, 588.
(10) Domb, C.; Barrett, A. J. *Polymer* **1976**, *17*, 179.
(11) Yamakawa, H.; Tanaka, G. *J. Chem. Phys.* **1967**, *47*, 3991.
(12) Einaga, Y.; Miyaki, Y.; Fujita, H. *J. Polym. Sci., Polym. Phys. Ed.* **1979**, *17*, 2103 (Part 9 of this series).
(13) Fox, T. G, Jr.; Flory, P. J. *J. Phys. Colloid Chem.* **1949**, *53*, 197.
(14) Shimada, J.; Yamakawa, H. *J. Polym. Sci., Polym. Phys. Ed.* **1978**, *16*, 1927.

Intrinsic Viscosity and Diffusion of Solutions of Flexible Polymer Molecules in Good Solvents

Robert Ullman

Research Staff, Ford Motor Company, Dearborn, Michigan 48121.
Received November 17, 1980

ABSTRACT: The steady-state hydrodynamics of flexible polymer molecules has been treated as a function of solvent power, using the Kirkwood and Kirkwood-Riseman methods with a chain statistics based on the "blob" hypothesis, refined, and smoothed to provide a physically realistic behavior. It provides an asymptotically accurate picture of the second moment of the distance between chain elements in good solvents, with a semiempirical fit in the range intermediate between good and bad solvents. We refer to the model as "quasi-blob" statistics to emphasize its relation to and deviation from the original "blob" model. Calculations of intrinsic viscosity, diffusion constant, radius of gyration, and hydrodynamic radius are performed and presented for several strengths of the excluded-volume interaction over a wide range of molecular weight. These have been compared with experiments on polystyrene solutions. The calculations and experiment are in fair agreement. Among the interesting results of the model are the following: (1) The exponent a in the expression $[\eta] = KM^a$ is a function of both molecular weight and the strength of the excluded-volume interaction. This is also seen in experiments if a large range of molecular weight (3 orders of magnitude or more) is used. (2) In a good solvent, a increases with molecular weight and then decreases. It can be greater than 0.8 in some cases. (3) Weill and des Cloizeaux[8] suggest that intrinsic viscosity and diffusion constants in good solvents approach the asymptotic molecular weight slowly because the hydrodynamic radius approaches this limit slowly. They suggest that the use of the formula $[\eta] \sim R_g^2 R_H/M$ in place of $[\eta] \sim R_g^3/M$ would account for the observed experimental behavior. Our calculations show a marginal advantage for the first of these two formulas.

Introduction

Viscosity and diffusion of polymers in solution provide useful information for characterization of macromolecules. The basis for the characterization rests on the solution of hydrodynamic equations for appropriate molecular models of a polymer chain. For the purpose of calculation, the polymer molecule is regarded as a macroscopic hydrodynamic body immersed in a solvent whose molecular structure is ignored. The solvent plays the role of a viscous fluid in which one or more polymer molecules are dispersed.

The polymer molecule is, on the other hand, treated as a microscopic body in the sense that its undergoes Brownian motion. Therefore, if the flow rate is sufficiently low, Brownian motion eliminates molecular and segmental orientation. It is this combination of the microscopic and

0024-9297/81/2214-0746$01.25/0

macroscopic that has proved so useful in the polymer flow problem.

In analyzing viscosity and diffusion, one treats the chain polymer molecule as a collection of segments distributed in space. It is crucial to the solution of the hydrodynamic problem that, no matter how dilute a polymer solution may be, the segments on an individual molecule are always near neighbors. Accordingly, the hydrodynamic interaction between pairs of segments plays a dominant role in the theory.

Normally, the solution of the flow equations for viscosity of a suspension requires that boundary values on the surface of the body be established. This is practical for objects of regular shape, such as a sphere or cylinder, but is not possible for a coiling polymer molecule with an irregular and ill-defined surface. To treat this difficulty, one replaces the polymer segment by a point force which acts on the fluid. The segmental friction constant supplies the proportionality between the point force and fluid velocity.

A general procedure for solving viscosity and diffusion problems based on the above ideas was developed by Kirkwood and Riseman[1] and Kirkwood,[2,3] and their methods have been extended and modified by numerous other investigators.[4–6]. A recent critical survey on the variety of techniques used with the Kirkwood method has been presented by Zimm.[7] In order to solve the Kirkwood–Riseman equations for intrinsic viscosity, the geometric arrangement of polymer segments must be specified. Once this is done, the calculations can be carried through, though, except for simple cases, numerical procedures rather than analytic methods are used.

The program to which this paper is devoted is to apply the Kirkwood–Riseman and Kirkwood equations to intrinsic viscosity of flexible-chain macromolecules in good solvents, that is, in cases where a substantial excluded-volume repulsion is anticipated. The results are to be compared with known experiments. The model of chain statistics adopted is based on the idea that excluded-volume interactions between pairs of chain segments are only significant if the segments are widely separated on the chain. This proposal has appeared under the enchanting name of the "blob" model, unfortunately in a form in which the introduction of the effective repulsion between segments varies too abruptly with chain spacing to be realistic.[8,9] Our modification of this hypothesis is in agreement with "blob" statistics at small and large segmental separation but makes the transition from one to the other limit smoothly and in accord with other known information. We refer to this as the quasi-blob model, to emphasize the connection with earlier formulations. It should be noted that since the excluded-volume problem has not been solved, except perhaps asymptotically, the details of the quasi-blob model are not supported by physical theory. Accordingly, our results are flawed by uncertainties in the chain statistics in the region intermediate between small and large excluded-volume effects. The ultimate test, however, is to determine the extent to which the model is in accord with experimental information.

Kirkwood–Riseman Model and Quasi-Blob Statistics

Attention is focused on a single polymer molecule, a linear chain composed of n Kuhn statistical elements.[10] In the absence of excluded-volume interactions, these elements are randomly oriented with respect to each other. The excluded-volume effect is a long-range correlation induced by an imbalance between forces of attraction and repulsion between pairs of chain elements.

For the purpose of calculation, we introduce a system of coordinates with an origin at the center of mass of the polymer molecule and spanned by a right-handed set of unit Cartesian vectors $\mathbf{i}$, $\mathbf{j}$, and $\mathbf{k}$. The vector from the center of mass to segment p is $\mathbf{R}_{0p}$, the vector connecting segment p to segment q is $\mathbf{R}_{pq}$, and the magnitude of a vector $\mathbf{R}$ is R. The solvent, a continuous fluid, undergoes laminar flow in the x direction; the velocity of the solvent, in the absence of a polymer molecule, is given by $\mathbf{v}^0 = \dot{\epsilon}(\mathbf{R}\cdot\mathbf{j})\mathbf{i}$, where $\dot{\epsilon}$ is the velocity gradient. The force exerted by the polymer molecule on the fluid is the sum of forces exerted by the segments. The force $\mathbf{F}_p$ exerted by segment p is proportional to the difference between the velocity of segment p and the velocity the fluid would have at $\mathbf{R}_{0p}$ if segment p were not there. The constant of proportionality is the segmental friction constant ζ.

By considering shearing stresses at a plane surface far from the polymer molecule, Kirkwood and Riseman, following an earlier calculation by Burgers[11] using a result of Oseen,[12] showed that the intrinsic viscosity, $[\eta]$, defined by

$$[\eta] = \lim_{c\to 0} (\eta - \eta_0)/\eta_0 c \tag{1a}$$

is given by

$$[\eta] = -(N_A/100M\eta_0\dot{\epsilon}) \sum_{p=1}^{n} \langle (\mathbf{R}_{0p}\cdot\mathbf{j})(\mathbf{F}_p\cdot\mathbf{i}) \rangle \tag{1b}$$

η_0 is the solvent viscosity in poise, η is the viscosity of the polymer solution, and c is the polymer concentration in grams per deciliter. N_A is Avogadro's number, M is the molecular weight of the polymer, and $\langle\ \rangle$ represents an ensemble average taken over a large number of molecules. A significant contribution to the proper calculation of forces depends on the hydrodynamic perturbations introduced by interactions between all pairs of segments of the chain.

At low velocities, the hydrodynamic equations are linear. The Oseen–Burgers[11,12] solutions as adopted by Kirkwood and Riseman lead to the expression

$$\langle (\mathbf{R}_{0q}\cdot\mathbf{j})(\mathbf{F}_p\cdot\mathbf{i}) \rangle = -(\zeta\dot{\epsilon}/6)\langle (\mathbf{R}_{0p}\cdot\mathbf{R}_{0q}) \rangle - (\zeta/6\pi\eta_0) \sum_{s=1}^{n}{}' \langle (\mathbf{R}_{0q}\cdot\mathbf{j})(\mathbf{F}_s\cdot\mathbf{i}) \rangle \langle R_{ps}^{-1} \rangle \tag{2}$$

Equation 2 is obtained if a number of simplifying assumptions are made. Brownian motion is assumed to be sufficiently effective that the polymer chain adopts a configuration identical with that in the absence of the flow field. The hydrodynamic interaction tensor is "preaveraged", which simplifies the mathematics. The preaveraging process has been shown in a few tractable cases to lead to small numerical changes in the final results.[13,14] $\sum'$ designates a sum over all terms except $p = s$.

Using a similar approach, Kirkwood[2,3] found that the diffusion constant may be obtained from the equation

$$D = (kT/\zeta)(n^{-1} + (\zeta/6\pi\eta_0)R_H^{-1}) \tag{3a}$$

$$R_H^{-1} = (1/n^2) \sum_{p,q}{}' \langle R_{pq}^{-1} \rangle \tag{3b}$$

T designates absolute temperature and k, the Boltzmann constant. The term n^{-1} in eq 3a is small and of negligible importance for polymers of high molecular weight.

The ensemble averages in eq 1b, 2, and 3 exhibit the dependence of diffusion and viscosity on chain configuration. In a flexible polymer molecule, the mean-square

distance between a pair of segments is given by

$$R_{pq}^2 = |p - q|^{2\nu}b^2 \quad (4)$$

where b is the segment length, $\nu = 0.5$ if there is no net excluded volume, and ν is close to 0.6 if the volume effect is large. A mean-field calculation yields $\nu = 0.6$;[15,16] $\nu = 0.588$ is the result obtained from a renormalization group analysis.[17]

In the quasi-blob model, $\nu = 0.5$ at low $|p - q|$ and is allowed to approach 0.6 as $|p - q|$ increases. The change of ν from 0.5 to 0.6 is temperature dependent. In addition, for small excluded volume, eq 4 is forced to match the perturbation theory of excluded volume:

$$\langle R_{pq}^2 \rangle = |p - q|b^2[1 + kf_{pq} + ...] \quad (5)$$

k is a constant, which appears here as a parameter of the problem, and f_{pq} is a complicated function of chain length and $|p - q|$ but is roughly of the order of $|p - q|^{1/2}$. In order to match eq 4 and 5 for $kf_{pq} \ll 1$, we set $1 + kf_{pq}$ equal to $\exp[kf_{pq}]$. The result is

$$\nu = 0.5(1 + kf_{pq}/\ln |p - q|) \quad (6)$$

a result which applies only at small $|p - q|$.

The extension of eq 6 to the domain of a large excluded volume is achieved by assuming

$$\nu = 0.6 - 0.1/(1 + P) \quad (7a)$$

$$P = \upsilon_e f_{pq}/\ln |p - q| \quad (7b)$$

By setting $p - q = n$, it may easily be shown that $\upsilon_e = 5zn^{-1/2}$, where z is the well-known excluded-volume parameter.[18] Equations 7a and 7b reduce to eq 6 ($\upsilon_e = 5k$) for small P. $\nu = 0.5$ if $P = 0$ and 0.6 if $P = \infty$. υ_e is temperature dependent and is assumed to take the form of

$$\upsilon_e = \beta_0(1 - \Theta/T) \quad (8)$$

Equation 8 meets the condition that excluded volume vanishes at the temperature $T = \Theta$, and it prescribes a temperature dependence similar to that prescribed in both mean-field and perturbation analyses of the volume effect.

The function f_{pq} of eq 6 is obtained by performing the prescribed calculations indicated in eq 9 of Fixman.[18] The result, found by replacing the sums in Fixman's eq 9 by integrals, is

$$(p - q)f_{pq} = (32/9)(p - q)^{3/2} - (4/9)p^{3/2} - (32/9)q^{3/2} - (32/9)(n - p)^{3/2} - (4/9)(n - q)^{3/2} + 4(n - p)(n - q)^{1/2} + 4p^{1/2}q - (4/3)(p - q)(n - q)^{1/2} - (4/3)(p - q)p^{1/2} + (4/3)(p - q)^2/n^{1/2} \quad (9)$$

This applies for $p > q$. If $q > p$, the symbols p and q are to be interchanged. In eq 2, the ensemble average $\langle \mathbf{R}_{0p} \cdot \mathbf{R}_{0q} \rangle$ is needed. This is obtained from the identity

$$\langle \mathbf{R}_{0p} \cdot \mathbf{R}_{0q} \rangle = 0.5(\sum_p \langle R_{pq}^2 \rangle/n + \sum_q \langle R_{pq}^2 \rangle/n - \langle R_{pq}^2 \rangle - 2R_g^2) \quad (10a)$$

where R_g^2, the centroidal radius of gyration, is given by

$$R_g^2 = \sum_p \langle R_{0p}^2 \rangle/n = \sum_{p,q} \langle R_{pq}^2 \rangle/2n^2 \quad (10b)$$

It is also evident from eq 2 that $\langle R_{pq}^{-1} \rangle$ is required for the calculation. In the absence of an excluded volume it is known that

$$\langle R_{pq}^{-1} \rangle = (6/\pi)^{1/2}\langle R_{pq}^2 \rangle^{-1/2} \quad (11)$$

It shall be assumed that this identity applies in the presence of an excluded volume as well.

In addition, for the purpose of comparison, a calculation of intrinsic viscosity was made, assuming that $\langle R_{pq}^2 \rangle = |p - q|^{1.2}b^2$ for all p and q. This is designated as the Peterlin model to relate it to an earlier suggestion of that author.[19]

Numerical Solutions of Intrinsic Viscosity and Diffusion Problems

The intrinsic viscosity is calculated by replacing sums by integrals, introducing reduced variables, and converting eq 1b to an integral and eq 2 to an integral equation. The integral equation is converted to a set of simultaneous linear equations by using Gaussian quadratures; these are solved, and the results are introduced into the expression for intrinsic viscosity, which is also integrated by Gaussian quadratures. The following substitutions are introduced:

$$x = 2p/n - 1 \quad (12a)$$

$$y = 2q/n - 1 \quad (12b)$$

$$t = 2s/n - 1 \quad (12c)$$

$$\phi(x,y) = -48(\mathbf{R}_{0q} \cdot \mathbf{j})(\mathbf{F}_p \cdot \mathbf{i})/(\zeta \dot{\epsilon} n b^2) \quad (12d)$$

$$f(x,y) = 8\langle(\mathbf{R}_{0q} \cdot \mathbf{R}_{0p})\rangle/(nb^2) \quad (12e)$$

$$K(x,t) = |x - t|^{-\nu}(0.5n)^{0.5-\nu} \quad (12f)$$

$$\zeta = 6\pi\eta_0 bQ \quad (12g)$$

$$\lambda = (3n/\pi)^{1/2}Q \quad (12h)$$

Q is a useful parameter by which the unknown segmental friction constant may be characterized. If the segmental friction constant were equal to that of a macroscopic sphere of diameter b, Q would be equal to 0.5. As we shall see, intrinsic viscosity is sensitive to Q only in the low molecular weight range.

Insertion of eq 12a–h in eq 1b and 2 yields

$$[\eta] = (\pi b^3 Q n N_A/1600M_0)\int_{-1}^{1} \phi(x,y)\, dx \quad (13a)$$

$$\phi(x,y) = f(x,y) - \lambda\int_{-1}^{1} \phi(t,y)K(x,t)\, dt \quad (13b)$$

M_0 is the molecular weight of a Kuhn statistical element.

The solution of eq 13b by Gaussian quadratures is very efficient but is a little difficult because $K(x,t)$ is singular (an integrable singularity) at $x = t$. We adapt a procedure of Ullman and Ullman[20] as modified by Schlitt.[21] This modification is based on rewriting

$$\int_{-1}^{1} K(x,t)\phi(t,y)\, dt = \int_{-1}^{1} K(x,t)[\phi(t,y) - \phi(x,y)]\, dt + g(x)\phi(x,y) \quad (14a)$$

$$g(x) = \int_{-1}^{1} K(x,t)\, dt \quad (14b)$$

Equation 13b takes the form

$$\phi(x,y) = f(x,y)/[1 + \lambda g(x)] - \lambda/[1 + \lambda g(x)]\int_{-1}^{1} [\phi(t,y) - \phi(x,y)]K(x,t)\, dt \quad (15)$$

The Gaussian quadrature method yields an excellent polynomial fit to an integral according to

$$\int_{-1}^{1} F(x)\, dx = \sum_{i=1}^{N} w_i F(x_i) \quad (16)$$

The statistical weights w_i and coordinates x_i are fixed once N is given. They are tabulated for many different

values of N.[22] Equation 15 takes the form

$$\sum_{k=1}^{N} A_{ik}\phi_{kj} = f_{ij}/(1 + \lambda g_i) \tag{17a}$$

where

$$A_{ik} = \lambda w_k K_{ik}/(1 + \lambda g_i) \qquad i \neq k \tag{17b}$$

$$A_{ii} = 1 - \sum_{k}{}' A_{ik} \tag{17c}$$

f_{ij}, K_{ik}, ϕ_k, and g_i are the discrete representations of $f(x,y)$, $K(x,t)$, $\phi(t,y)$, and $g(x)$ at the points x_i, x_j, and x_k. Inversion of the matrix $\{A_{ik}\}$ leads to

$$\phi_{kj} = \sum_{i=1}^{N} A_{ki}^{-1} f_{ij}/(1 + \lambda g_i) \tag{18a}$$

and

$$[\eta] = \pi b^3 n N_A Q \sum_{i=1}^{N} w_i \phi_{ii}/1600 M_0 \tag{18b}$$

Viscosity integral equations similar to eq 13b have been solved by eigenfunction methods,[23] and these solutions are preferable for calculations of dynamical properties in order to extract normal modes of motion. For the steady-state problem, the direct numerical methods have an advantage over an expansion in a series of eigenfunctions in that results of the calculation are obtained more easily, and there is no need for projecting out the separable modes of motion.

It is evident that a calculated value of $[\eta]$ from eq 18b is a function of the number of divisions N used in estimating integrals, the errors being dependent on the magnitude of the determinant of A_{ij}. The results become exact as N approaches infinity. In calculating intrinsic viscosity, we have taken N to be 20, 40, and 80, plotted the results vs. N^{-1}, and extrapolated to $N^{-1} = 0$. The variation with N yields a measure of the magnitude of numerical errors, which tend to be of the order of 0.1% but increase with molecular weight of the polymer and with the magnitude of the excluded-volume parameter, v_e.

In eq 7b, P is a slowly increasing function of $|p - q|$ for $|p - q| \geq 8$. From the nature of the physical problem, it is clear that P must increase monotonically, and this is not so for $|p - q| \leq 7$. (Note that $x^{1/2}/\ln x$ is a minimum at $x = e^2$.) We adjust our calculation by redefining P for small $|p - q|$ by

$$P = v_e f_{pq}/\ln 7 \quad \text{for} \quad |p - q| \leq 7 \tag{19}$$

Otherwise eq 7b still applies.

Both the hydrodynamic radius, R_H (eq 3b), and the radius of gyration (eq 10b) have been calculated by quasi-blob statistics, and the diffusion constant has been computed from R_H (eq 3a). The sums in the equations are very lengthy if the molecular weight of the polymer is high. For computational purposes, we have introduced the following approximations:

$$R_g^2 = \frac{1}{2n^2}\sum_{p,q=1}^{M}{}' \langle R_{pq}^2\rangle + \int_0^n\int_0^n \langle R_{pq}^2\rangle \, dp\, dq - \int_0^M\int_0^M \langle R_{pq}^2\rangle \, dp\, dq \tag{20a}$$

$$R_H^{-1} = \frac{1}{n^2}\sum_{p,q=1}^{M}{}' \langle R_{pq}^{-1}\rangle + \int_0^n\int_0^n \langle R_{pq}^{-1}\rangle \, dp\, dq - \int_0^M\int_0^M \langle R_{pq}^{-1}\rangle \, dp\, dq \tag{20b}$$

M is a number of the order of 50 or 100. Neither R_g nor R_H varies appreciably if M is taken to be 50 or greater. The integrals are calculated by quasi-blob statistics and Gaussian quadratures. R_g is insensitive to N (the number of terms in the Gaussian quadrature), but R_H is determined by extrapolating to N^{-1} equal zero, as was done in calculating intrinsic viscosity. Errors in R_H were generally of the order of 0.1% but became larger with increasing molecular weight and increasing excluded volume.

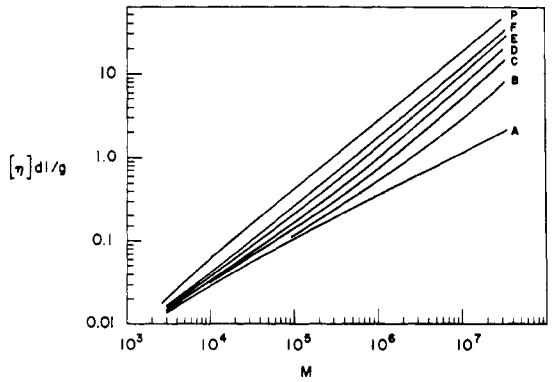

Figure 1. Plot of $[\eta]$ vs. M on a log-log scale based on quasi-blob statistics: (A) $v_e = 0$; (B) $v_e = 0.02$; (C) $v_e = 0.05$; (D) $v_e = 0.1$; (E) $v_e = 0.2$; (F) $v_e = 0.4$; (P) Peterlin model with $\nu = 0.6$. $Q = 0.5$.

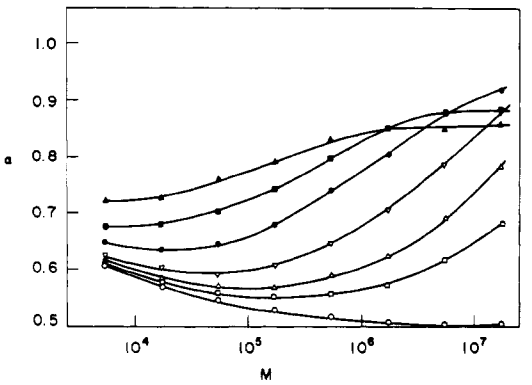

Figure 2. Mark-Houwink exponent a as a function of M: (○) $v_e = 0$; (□) $v_e = 0.005$; (△) $v_e = 0.01$; (▽) $v_e = 0.02$; (●) $v_e = 0.05$; (■) $v_e = 0.1$; (▲) $v_e = 0.2$. $Q = 0.5$.

Numerical Results

Intrinsic viscosity calculations using the quasi-blob model were carried out for polymers over a wide range of molecular weight, for several values of the excluded-volume interaction strength, and for two values of Q. The bond length b and monomer molecular weight M_0 were taken to be 5 Å and 100 daltons, respectively. Results are given in Table I. Table II contains results of the calculation of the Peterlin model. Figure 1 contains a number of plots of log $[\eta]$ vs. log M taken from data in Tables I and II.

It is clear from Figure 1 that the parameter a in the Mark-Houwink equation, $[\eta] = KM^a$, is not a constant, though deviations from a straight line in a log-log plot are small if the range of molecular weight is small. It is particularly interesting that some of the curves for part of the range of molecular weight have slopes greater than that seen for the Peterlin model. This is seen clearly in Figure 2, where a is plotted vs. molecular weight, and in Figure 3, where a is plotted vs. v_e. The fact that a is greater than 0.8 in some cases is surprising. However, since the intrinsic viscosity-molecular weight relation approaches that of Θ solvent ($[\eta] \sim M^{0.5}$) at low molecular weight and the corresponding curve for a Peterlin model ($[\eta] \sim M^{0.8}$) at high molecular weight, it must pass through a region where a is greater than 0.8. A similar phenomenon has been

Table I
Intrinsic Viscosity as a Function of Molecular Weight and Excluded-Volume Parameter

	M								
v_e	3×10^3	10^4	3×10^4	10^5	3×10^5	10^6	3×10^6	10^7	3×10^7
				$Q = 0.5$					
0	0.01360	0.02828	0.05289	0.1021	0.1824	0.3398	0.5943	1.090	1.895
0.002	0.01363	0.02837	0.05327	0.1035	0.1869	0.3554	0.6409	1.251	2.384
0.004	0.01366	0.02855	0.05390	0.1052	0.1919	0.3717	0.6904	1.424	2.930
0.005	0.01367	0.02859	0.05394	0.1057	0.1937	0.3787	0.7122	1.497	3.165
0.008	0.01375	0.02886	0.05473	0.1087	0.2013	0.4034	0.7883	1.756	4.025
0.01	0.01377	0.02896	0.05548	0.1096	0.2048	0.4173	0.8312	1.913	4.512
0.02	0.01393	0.02957	0.05736	0.1168	0.2274	0.4944	1.073	2.759	7.233
0.03	0.01404	0.03011	0.05905	0.1237	0.2488	0.5662	1.294	3.532	9.549
0.04	0.01416	0.03069	0.06095	0.1302	0.2688	0.6358	1.513	4.273	11.63
0.05	0.01430	0.03125	0.06291	0.1365	0.2878	0.7017	1.700	4.874	13.34
0.06	0.01440	0.03177	0.06430	0.1424	0.3071	0.7609	1.876	5.393	14.75
0.08	0.01462	0.03203	0.06756	0.1536	0.3408	0.8727	2.204	6.385	17.16
0.1	0.01483	0.03353	0.07060	0.1643	0.3711	0.9677	2.465	7.138	18.88
0.12	0.01503	0.03436	0.07328	0.1734	0.3987	1.055	2.703	7.760	20.42
0.2	0.01567	0.03716	0.08248	0.2056	0.4875	1.321	3.358	9.304	23.82
0.3	0.01629	0.03970	0.9105	0.2325	0.5633	1.536	3.854	10.54	26.40
0.4	0.01679	0.04176	0.09748	0.2526	0.6153	1.662	4.128	11.08	27.61
0.5	0.01715	0.04335	0.1025	0.2680	0.6511	1.746	4.323	11.70	28.34
0.7	0.01774	0.04566	0.1098	0.2895	0.7081	1.878	4.567	12.36	29.36
				$Q = 0.25$					
0	0.01089	0.02427	0.04774	0.09568	0.1750	0.3318	0.5860	1.083	1.887
0.002	0.01090	0.02441	0.04830	0.09757	0.1804	0.3484	0.6378	1.253	2.357
0.004	0.01092	0.02451	0.04865	0.09898	0.1848	0.3637	0.6844	1.417	2.914
0.005	0.01094	0.02457	0.04884	0.09968	0.1872	0.3717	0.7088	1.494	3.181
0.008	0.01097	0.02474	0.04937	0.1017	0.1930	0.3945	0.7771	1.750	4.002
0.01	0.01100	0.02484	0.04979	0.1030	0.1976	0.4092	0.8260	1.918	4.567
0.02	0.01111	0.02537	0.05163	0.1097	0.2189	0.4834	1.061	2.763	7.271
0.03	0.01122	0.02587	0.05335	0.1163	0.2393	0.5532	1.279	3.512	9.513
0.04	0.01132	0.02633	0.05503	0.1224	0.2591	0.6238	1.497	4.237	11.54
0.05	0.01144	0.02682	0.05671	0.1282	0.2785	0.6886	1.682	4.843	13.28
0.06	0.01154	0.02727	0.05827	0.1337	0.2956	0.7446	1.854	5.353	14.74
0.08	0.01172	0.02805	0.06109	0.1446	0.3279	0.8564	2.167	6.318	17.00
0.1	0.01189	0.02891	0.06387	0.1545	0.3584	0.9579	2.473	7.089	18.98
0.12	0.01206	0.02959	0.06632	0.1627	0.3854	1.038	2.668	7.648	20.15
0.2	0.01264	0.03209	0.07482	0.1925	0.4712	1.287	3.298	9.245	23.35

Table II
Intrinsic Viscosity as a Function of Molecular Weight: Peterlin Model

M	$Q = 0.25$	$Q = 0.5$
3×10^3	0.01719	0.02092
10^4	0.05210	0.06001
3×10^4	0.1385	0.1531
10^5	0.3912	0.4187
3×10^5	0.9854	1.035
10^6	2.672	2.761
3×10^6	6.597	6.737
10^7	17.57	17.79
0×10^7	42.66	42.98

noted by François et al.[24] for the radius of gyration.

If the flow of solvent through the domain occupied by segments of a polymer molecule were inappreciable by comparison with flow around the coil, $[\eta]$ would be independent of the segmental friction constant. This limit of the impermeable coil is to be constrasted with a partially free-draining model in which flow through the polymer coil is appreciable. In Figure 4, a plot of $[\eta](Q = 0.5)/[\eta](Q = 0.25)$ is shown. A ratio of unity would indicate an impermeable molecule. It is evident that the polymer molecule becomes impermeable at high molecular weight but is far from the limit in the lower molecular weight range. The data in the figure are taken from calculated results at the Θ condition; however, very similar curves are obtained at all values of excluded volume.

The increasing sensitivity of the intrinsic viscosity to excluded-volume interactions as a function of molecular weight is exhibited in plots of the ratio $[\eta](v_e)/[\eta](v_e = 0)$

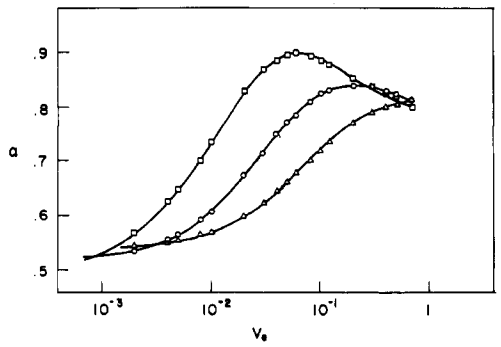

Figure 3. Mark–Houwink exponent a for three different molecular weight intervals. ($a = \log [\eta]_2/\log [\eta]_1$): (△) $M_1 = 3 \times 10^4$, $M_2 = 3 \times 10^5$; (○) $M_1 = 3 \times 10^5$, $M_2 = 3 \times 10^6$; (□) $M_1 = 3 \times 10^6$, $M_2 = 3 \times 10^7$. $Q = 0.5$.

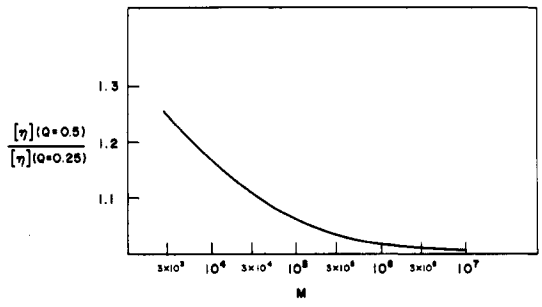

Figure 4. Effect of segmental friction constant on intrinsic viscosity, $[\eta](Q = 0.5)/[\eta](Q = 0.25)$, vs. M.

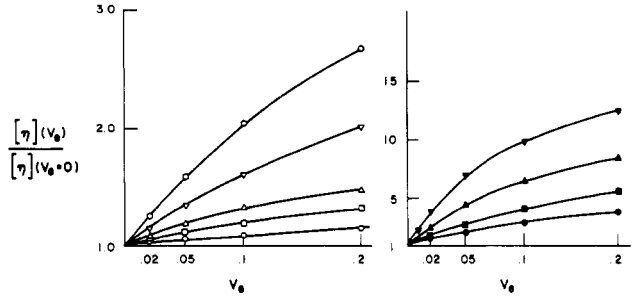

Figure 5. Change in intrinsic viscosity plotted as the ratio $[\eta](\upsilon_e)/[\eta](\upsilon_e = 0)$ as a function of υ_e plotted for several values of molecular weight: (○) $M = 3 \times 10^3$; (□) $M = 10^4$; (△) $M = 3 \times 10^4$; (▽) $M = 10^5$; (○) $M = 3 \times 10^5$; (●) $M = 10^6$; (■) $M = 3 \times 10^6$; (▲) $M = 10^7$; (▼) $M = 3 \times 10^7$. $Q = 0.5$.

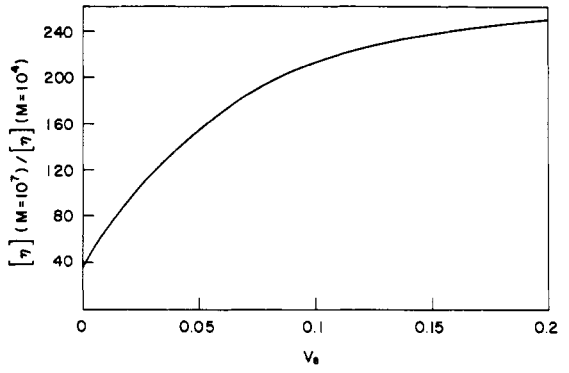

Figure 6. Plot of the ratio $[\eta](M = 10^7)/[\eta](M = 10^4)$ vs. υ_e. $Q = 0.5$.

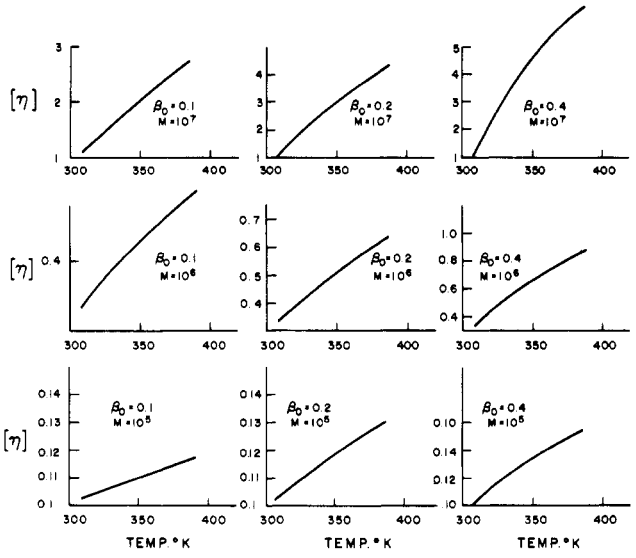

Figure 7. Graphs of $[\eta]$ vs. temperature for three values of molecular weight and for three values of the excluded-volume parameter β_0 (see eq 8). $Q = 0.5$, $\Theta = 308$ K.

vs. molecular weight in Figure 5.

The ratio of $[\eta](M_2)/[\eta](M_1)$ for M_2 greater than M_1 increases with increasing υ_e. This is shown in Figure 6.

Figure 7 contains calculated values of intrinsic viscosity vs. temperature, using three different values of β_0, a parameter which measures the strength of repulsive forces between segments. For convenience, Θ was taken equal to 35 °C. Changes of intrinsic viscosity with temperature increase with increasing molecular weight.

It follows from the Kirkwood–Riseman model and random flight statistics that the intrinsic viscosity is proportional of R_g^3/M for an impermeable coil.

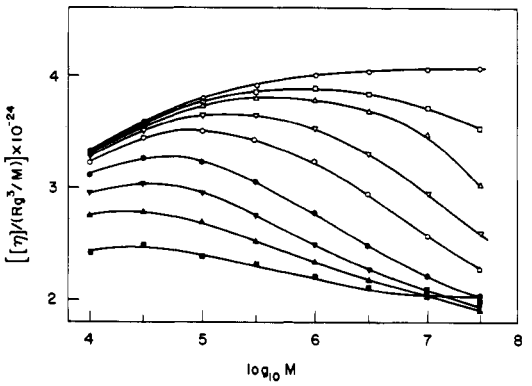

Figure 8. Variation of $[\eta]/(R_g^3/M)$ with molecular weight for several values of υ_e: (○) $\upsilon_e = 0$; (□) $\upsilon_e = 0.002$; (△) $\upsilon_e = 0.005$; (▽) $\upsilon_e = 0.01$; (○) $\upsilon_e = 0.02$; (●) $\upsilon_e = 0.05$; (▼) $\upsilon_e = 0.1$; (▲) $\upsilon_e = 0.2$; (■) $\upsilon_e = 0.7$. $Q = 0.5$.

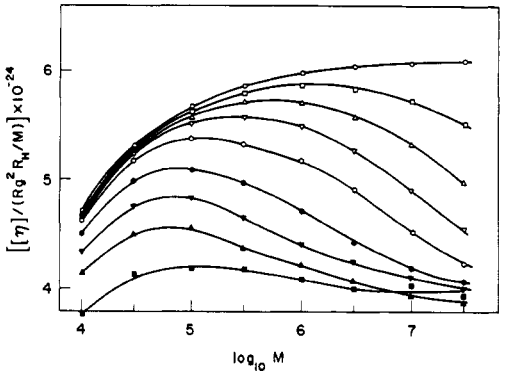

Figure 9. Variation of $[\eta]/(R_g^2R_H/M)$ with molecular weight for several values of υ_e: (○) $\upsilon_e = 0$; (□) $\upsilon_e = 0.002$; (△) $\upsilon_e = 0.005$; (▽) $\upsilon_e = 0.01$; (○) $\upsilon_e = 0.02$; (●) $\upsilon_e = 0.05$; (▼) $\upsilon_e = 0.1$; (▲) $\upsilon_e = 0.2$; (■) $\upsilon_e = 0.7$. $Q = 0.5$.

It had been suggested by Flory[15,25] that intrinsic viscosity varies with R^3/M for coiled macromolecules in general, where R is a reasonable linear dimension of the polymer molecule. Flory, in his own work used the root-mean-square end-to-end distance of the chain, that is, $\langle R_N^2\rangle^{3/2}/M$; others have preferred R_g^3/M.

Recently, arguing in terms of the blob model, Weill and des Cloizeaux[8] have suggested the fact that a in $[\eta] = KM^a$ is often less than 0.8 arises from the appearance of R_H in the viscosity model and the slow approach of R_H to its asymptotic value at high molecular weight. They propose the proportionality $[\eta] \sim R_g^2R_H/M$. To address this question, we have presented plots of $[\eta]/(R_g^3/M)$ vs. M in Figure 8 and $[\eta]/(R_g^2R_H/M)$ vs. M in Figure 9. In both cases at $T = \Theta$ ($\upsilon_e = 0$), the ratios approach a constant at high molecular weight. Deviation from this limit at low molecular weight arises from a partial free draining of the polymer molecule. The excluded-volume interaction has an appreciable influence on these ratios. $[\eta]/(R_g^2R_H/M)$ approaches a limit at high molecular weight only for large υ_e in the experimentally interesting range.

The ratio $[\eta]/(R_g^3/M)$ varies more with molecular weight than $[\eta]/(R_g^2R_H/M)$, but the difference does not appear to be highly significant. Both of the ratios vary with molecular weight by a factor of 2 or less in a molecular weight range where $[\eta]$ varies by several hundred or a thousand.

Calculations of R_g and R_H are listed in Table III. Plots of log diffusion constant vs. log molecular weight are shown in Figure 10. The log D vs. log M curves are slightly nonlinear, but less so than is found for intrinsic viscosity. The reason for this is the following. The nonlinearity at

Table III
Molecular Dimensions as a Function of Molecular Weight and Excluded Volume

	M								
v_e	3×10^3	10^4	3×10^4	10^5	3×10^5	10^6	3×10^6	10^7	3×10^7
				R_g					
0.00	11.17	20.41	35.35	64.53	111.8	204.1	353.5	645.3	1118
0.002	11.19	20.46	35.50	65.05	113.3	209.2	368.7	695.7	1267
0.005	11.21	20.54	35.73	65.81	115.6	216.6	390.3	764.9	1464
0.01	11.25	20.66	36.10	67.02	119.1	228.0	423.0	865.6	1735
0.02	11.32	20.91	36.81	69.31	125.7	248.3	478.2	1023	2122
0.03	11.39	21.14	37.47	71.40	131.5	265.6	522.7	1140	2381
0.04	11.45	21.36	38.10	73.33	136.7	280.5	559.2	1230	2566
0.05	11.52	21.57	38.68	75.11	141.5	293.4	589.6	1300	2704
0.06	11.58	21.76	39.24	76.76	145.7	304.8	615.3	1357	2811
0.08	11.69	22.13	40.26	79.72	153.2	323.8	656.3	1443	2965
0.1	11.79	22.47	41.17	82.30	159.4	338.9	687.5	1505	3071
0.12	11.89	22.78	41.99	84.56	164.7	351.3	712.1	1552	3149
0.2	12.22	23.80	44.60	91.38	179.9	384.3	773.3	1662	3322
0.3	12.53	24.73	46.87	96.88	191.2	406.8	812.2	1727	3420
0.4	12.76	25.41	48.46	100.5	198.3	420.3	834.3	1763	3472
0.5	12.95	25.93	49.65	103.2	203.2	429.2	848.6	1785	3505
0.7	13.22	26.67	51.30	106.7	209.5	440.3	866.0	1812	3543
				R_H					
0.00	9.278	14.37	23.79	43.08	74.51	136.1	235.6	430.1	744.9
0.002	9.286	14.40	23.86	43.30	75.10	138.2	242.2	451.7	808.7
0.005	9.298	14.43	23.95	43.64	76.17	141.3	251.4	481.1	890.7
0.01	9.317	14.49	24.12	44.16	77.70	146.3	265.2	522.7	1000
0.02	9.354	14.60	24.43	45.14	80.58	154.8	288.1	587.0	1156
0.03	9.389	14.70	24.72	46.03	82.96	162.1	306.5	634.9	1263
0.04	9.422	14.80	25.00	46.85	85.16	168.3	321.7	671.7	1340
0.05	9.454	14.87	25.24	47.04	87.14	173.7	342.7	701.1	1396
0.06	9.484	14.97	25.49	48.29	88.93	178.5	345.0	725.2	1444
0.08	9.541	15.15	25.90	49.53	92.03	186.3	362.2	763.0	1510
0.1	9.593	15.28	26.28	50.51	94.63	192.7	375.6	789.4	1558
0.12	9.641	15.41	26.61	51.55	96.90	198.0	386.1	810.2	1593
0.2	9.801	15.83	27.78	54.35	103.2	212.1	413.1	860.0	1674
0.3	9.948	16.21	28.57	56.60	107.9	222.1	430.8	890.5	1719
0.4	10.06	16.46	29.20	58.12	110.9	228.1	441.1	907.2	1744
0.5	10.14	16.67	29.67	59.18	113.1	232.1	447.7	918.1	1760
0.7	10.27	16.97	30.30	60.62	115.8	237.1	456.0	931.0	1780

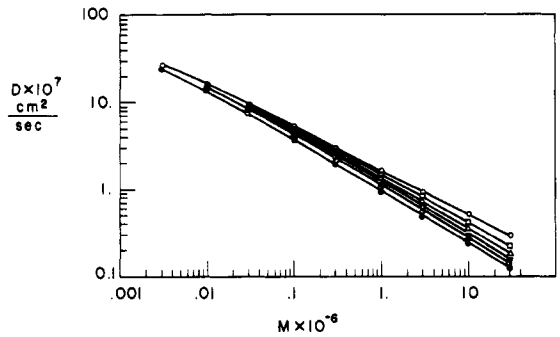

Figure 10. Variation of the diffusion constant with molecular weight on a log–log basis: (○) $v_e = 0$; (□) $v_e = 0.01$; (△) $v_e = 0.03$; (▽) $v_e = 0.1$; (○) $v_e = 0.2$; (●) $v_e = 0.5$. $Q = 0.5$.

higher molecular weights depends on the nonlinearity of log R with log M, where R is a characteristic chain dimension. D varies with R^{-1} and $[\eta]$ with R^3, thus leading to greater sensitivity to excluded-volume interactions in $[\eta]$ than in D.

Comparison with Experiment

The calculated results presented in the tables are based on a hypothetical length of a statistical element $b = 5$ Å and a hypothetical molecular weight of the element M_0, equal to 100 daltons. To use the calculated tables for comparison with experiment, the measured results must be reduced by an appropriate scaling factor. Thus $[\eta]^*$, the reduced intrinsic viscosity, is given by

$$[\eta]^* = 1.25[\eta]_{\text{exptl}}/(b^3/M_0) \quad (21)$$

$[\eta]_{\text{exptl}}$ is the measured result, b is the length of a Kuhn element, and M_0 is its molecular weight. The value 1.25 for b^3/M_0 has been used in developing the tables, and $[\eta]^*$ is the scaled experimental result. The scaled molecular weight of a Kuhn element is equal to the molecular weight of a monomer multiplied by the ratio b(Kuhn element)/b(monomer). The determination of b for a Kuhn statistical element is achieved here by identification of the chain length and radius of gyration with the appropriate parameters

$$L = Nb \quad (22a)$$

$$R_g^2 = Nb^2/6 \quad (22b)$$

L being the length of the extended polymer molecule and N the number of statistical elements per molecule. Equation 22b is valid under the Θ condition only. Data suitable for determination of N and b are compiled for a numer of well-known polymers by Yamakawa.[26]

It has been suggested by Akcasu et al.[27] that b changes with excluded volume in accord with certain scaling laws. This refinement is not introduced in our analysis. We adhere to the usual assumption that b, determined at Θ conditions, remains unchanged with changes in the solvent–polymer interaction.

For purposes of comparison with experiments, we will consider intrinsic viscosity measurements of polystyrene in cyclohexane and benzene. Data are taken from the dissertation of Slagowski[28] and from publications of Altares et al.,[29] Yamaguchi et al.,[30] and Einaga et al.[31] Since Slagowski's work is not published in the open literature,

Table IV
Some Results from Slagowski's Thesis[28]

polymer name	$M_w \times 10^{-6}$	M_z/M_w[a]	$[\eta]$, dL/g cyclohexane 35.4 °C	cyclohexane 45 °C	cyclohexane 55 °C	benzene 40 °C
LJF13	43.7	1.11	5.5	12.7	15.8	68
LJF18	27.3	1.18	4.4	9.12	10.85	36.5
D-I-1-1	9.6	1.10	2.35	4.29	5.15	14.4
WA61970	1.68	1.10	1.22	1.57	1.75	3.83
WA25166	0.411	1.09	0.570	0.684	0.735	1.34

[a] This ratio was calculated by sedimentation equilibrium.

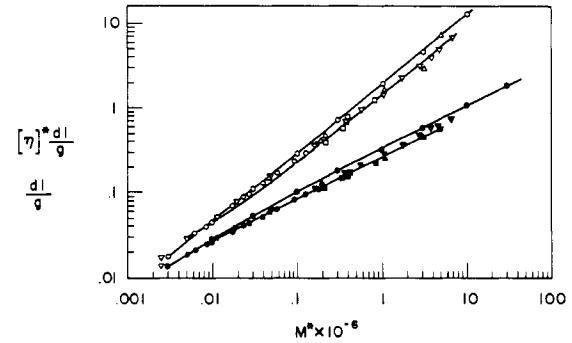

Figure 11. Comparison of experimental and calculated intrinsic viscosities as a function of molecular weight: (○) calculated from quasi-blob model, $v_e = 0.07$, $Q = 0.5$; (●) calculated for $v_e = 0$, $Q = 0.5$, the Gaussian model to apply at $T = \Theta$; (△) Slagowski, polystyrene in benzene at 40 °C; (○) Altares et al., polystyrene in benzene at 30 °C; (□) Yamaguchi et al., polystyrene in benzene at 35 °C; (▽) Einaga et al., polystyrene in benzene at 25 °C; (▲) Slagowski, polystyrene in cyclohexane at 35.4 °C; (●) Altares et al., polystyrene in cyclohexane at 34.5 °C; (■) Yamaguchi et al., polystyrene in cyclohexane at 34.5 °C; (▼) Einaga et al., polystyrene in cyclohexane at 34.5 °C. The uppermost curve is fitted to the calculated points at $v_e = 0.7$; the second from top is fitted to the experiments on polystyrene in benzene; the third is fitted to the calculated points at $v_e = 0$; the bottom curve is fitted to the experiments on polystyrene in cyclohexane at the Θ temperature.

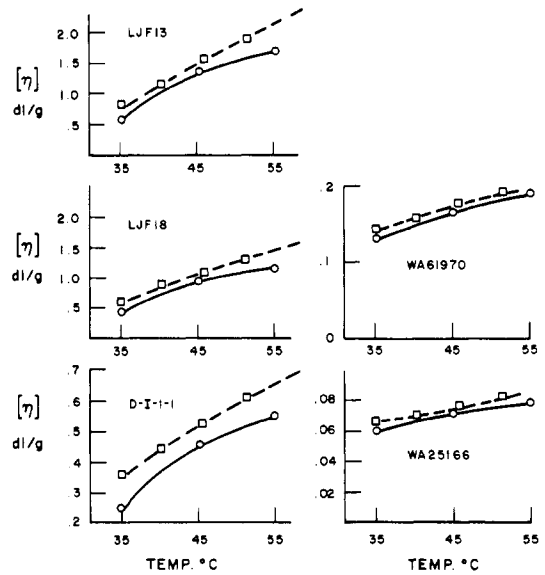

Figure 12. Variation of intrinsic viscosity with temperature: (---) calculated from quasi-blob model; (—) experiments of Slagowski, $\beta_0 = 0.6$, $Q = 0.5$. The names refer to samples of Table IV. Θ = 35 C.

a brief summary of his measurements is given in Table IV. Data on diffusion of polystyrene in cyclohexane and 2-butanone are taken from the work of King et al.[32,33] An equation relating diffusion constant to molecular weight for polystyrene in benzene from Adam and Delsanti[34] is the source of data on that system.

Diffusion data can be placed on a reduced basis by taking into account that $R_H^* = R_H(5/b)$, where R_H is a measured hydrodynamic radius and R_H^* a reduced radius which can be compared with calculations in Table III.

The Yoon–Flory parameters on polystyrene are adopted here.[35] The C–C bond length is 1.53 Å and the average CCC bond angle is 113°. It follows that the chain length L equals $0.0245/M$. Light scattering measurements at the Θ point yield $R_g^2 = 0.088M$.[36] Equations 22a and 22b yield $b = 21.54$ Å; there are 8.45 monomer units per statistical element, and M_0 is 880. $[\eta]^* = 0.1101[\eta]_{exptl}$ and $M^* = 0.1184M$.

The rescaled data on viscosity, taken from ref 28–31, are presented in Figure 11. The trend with molecular weight in experiment and calculation is in reasonable agreement, though the absolute values differ. There are a number of reasons why close numerical agreement between calculation and experiment are not to be expected from the Kirkwood–Riseman model, some of which are mentioned in the earlier sections of this paper. The recent study by Zimm[7] gives a good overview of the problem plus some reasonable estimates of the magnitude of the errors involved. It is also evident that the choice of the bond length b controls the scaling of the data. If this choice is in error, the absolute magnitudes of the calculation and experiment will be relatively displaced.

Two noteworthy facts are evident in Figure 11. First of all, the upward curvature of the log $[\eta]$ vs. log M plot is apparent in both experiment and theory for the polystyrene–benzene solution. The plots of $[\eta]$ in cyclohexane at $T = \Theta$ are straight at high molecular weight as expected, but the downward curvature of the theoretical plots at low molecular weight is not seen in the experiment. The downward curvature in the theory results from the partial free draining of the polymer coil. Its absence in the experiment may signal a breakdown in the method. As mentioned earlier, the hydrodynamic argument is based on treating a polymer molecule as a macroscopic body in a solvent which is a continuous fluid. This assumption becomes invalid as the molecular weight of the polymer decreases.

Figure 12 contains plots of intrinsic viscosity vs. temperature for polystyrene in cyclohexane taken from Slagowski (Table IV). The agreement is good, with the experimental results exhibiting slightly more curvature than the theoretical plots. The same constant β_0 (eq 8) is used for all polystyrene samples, independent of molecular weight. The accord between experimental and calculated results constitutes further support for the quasi-blob model.

Figure 13 compares the experimental data of King et al. and the equation (arrived at from experiments) of Adam

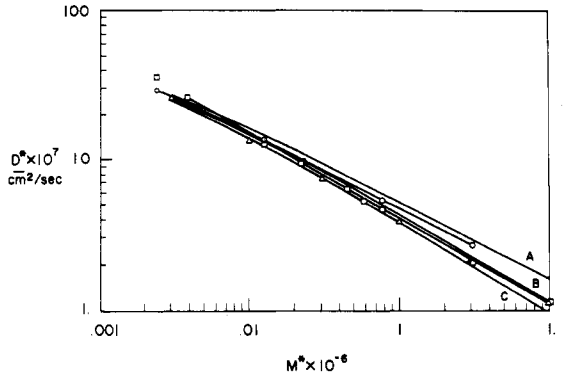

Figure 13. Comparison of experimental and calculated diffusion constants as a function of molecular weight. Curve A, calculated for a Θ solvent; curve B, calculated for $v_e = 0.12$; curve C, calculated for $v_e = 0.7$. (○) experiments of King et al., polystyrene in cyclohexane at $T = 35$ °C; (□) experiments of King et al., polystyrene in 2-butanone at 25 °C; (△) experiments of Adam and Delsanti, polystyrene in benzene at 20 °C.

and Delsanti with the calculations. Agreement is good, but the relative insensitivity of diffusion constant to excluded-volume interactions makes this a less critical test of the theory than is the viscosity.

The Kuhn statistical length, b, is obtainable from experiment, but nevertheless it would be preferable to express the results directly in terms of measurable quantities. This is easily achieved at the Θ temperature. Expressing n and b in terms of the radius of gyration, we write eq 13a as

$$[\eta] = 6^{3/2}\pi N_A R_g^3 \left[Q n^{1/2} \int_{-1}^{1} \phi(x,y)\, dx \right] \Big/ (1600M) \qquad (23)$$

The term in the square brackets tends to a constant value as M gets large. This is seen easily from the plot of $[\eta]/(R_g^3/M)$ of Figure 8 at $v_e = 0$.

A comparable formula for the excluded-volume case would be

$$[\eta] = 6^{3/2}\pi^{1/2} N_A R_g^2 R_H \times \left[Q n^{0.2} \int_{-1}^{1} \phi(x,y)\, dx / f_g(n) f_H(n) \right] \Big/ (1600M) \qquad (24a)$$

$$R_g^2 = n^{1.2} b^2 f_g(n)/6 \qquad (24b)$$

$$R_H = n^{0.6} b f_H(n) (\pi/6)^{1/2} \qquad (24c)$$

Equations 24a–c are equivalent to eq 13a. The usefulness of this formulation is that $[\eta]$, R_g, R_H, and M are measurable, and the term in the brackets is insensitive to n for reasonably high molecular weight in good solvents. In Table V, calculations are presented which show the variation of the bracketed terms with n at the Θ point and in good solvents.

Table V
Asymptotic Behavior at High Molecular Weight

	v_e		
n	X_Θ [a] = 0.00	X_v [b] = 0.12	X_v [b] = 0.70
30	1.615	3.30	2.96
100	1.828	4.28	3.77
300	1.977	4.66	4.13
1 000	2.075	4.69	4.16
3 000	2.141	4.54	4.14
10 000	2.177	4.29	4.06
30 000	2.198	4.12	4.01
100 000	2.213	3.88	3.98
300 000	2.222	3.85	3.93

[a] $X_\Theta = (3n/\pi)^{1/2} Q \int_{-1}^{1} \phi(x,x)\, dx$ (see eq 23). [b] $X_v = (3/\pi)^{1/2} Q n^{0.2} \int_{-1}^{1} \phi(x,x)\, dx / [f_g(n) f_H(n)]$ (see eq 24b).

Discussion

The quasi-blob chain statistics used to represent polymer chains in good solvents is generally successful in fitting experimental data on intrinsic viscosities and diffusion constants. Both the theoretical calculation of intrinsic viscosity and careful experiments carried out over a wide range of molecular weight[31] (see Figure 11) show an upward curvature in a log $[\eta]$ vs. log M plot. The variation of intrinsic viscosity with temperature near the Θ point is in accord with the calculation as well over a wide range with molecular weight. The log D vs. log M plots are also in good accord, but the relatively moderate dependence of D on changes in dimension of the polymer molecule does not provide a sensitive test of the calculation.

The faults are primarily at low molecular weight, where the slope of the calculated curve is steeper than the experiments show. There are at least two possible sources for this discrepancy. One is that the Kuhn statistical element is represented by a point which exerts a force on the fluid. Hydrodynamic interactions within a segment are not considered in such a model, but, for example, a Kuhn element has a molecular weight of 880 for polystyrene, and hydrodynamic interactions between monomer units within the Kuhn element exist in the real polymer solution but not in the calculation. The relative importance of intraelement hydrodynamic forces decreases with increasing molecular weight of the polymer.

In most calculations of hydrodynamics of polymer solutions, the polymer molecule is treated as a macroscopic object in a continuous fluid. This picture, valid at high molecular weight, begins to break down as the molecular weight becomes sufficiently low. A polystyrene of molecular weight 30 000 is composed of 34 Kuhn elements. The particle-in-a-fluid picture may begin to show discrepancies at this stage and certainly breaks down completely as the molecular weight of the polymer becomes comparable with that of the solvent.

The quasi-blob chain statistics is designed to be consistent with theoretical expectations for segments on a polymer chain which are close to each other in chain space and for segments which are widely separated. Intermediate distances are estimated by a smoothly varying but arbitrary formula. An accurate estimate of errors in the results arising from this source is not available, but we believe these errors to be small.

In summary, we present these calculations to supply a systematic procedure for the interpretation of intrinsic viscosity and diffusion constants determined in good solvents. The uncertainties in the analysis have been pointed out. Application of the model to other problems of polymer hydrodynamics, such as rotatory diffusion, dielectric relaxation, dynamic birefringence, and dynamic mechanical properties, remains to be accomplished.

Acknowledgment. The author is grateful to A. Z. Akcasu and W. H. Stockmayer for helpful suggestions on the chain statistics of the model.

References and Notes

(1) Kirkwood, J. G.; Riseman, J. *J. Chem. Phys.* **1948**, *16*, 565.
(2) Kirkwood, J. G. *Recl. Trav. Chim. Pays-Bas* **1949**, *68*, 649.
(3) Kirkwood, J. G. *J. Polym. Sci.* **1954**, *12*, 1.
(4) Rouse, P. E., Jr. *J. Chem. Phys.* **1953**, *21*, 1272.
(5) Zimm, B. H. *J. Chem. Phys.* **1956**, *24*, 269.
(6) Fixman, M. *J. Chem. Phys.* **1966**, *45*, 785, 793.
(7) Zimm, B. H. *Macromolecules* **1980**, *13*, 592.
(8) Weill, G.; des Cloizeaux, J. *J. Phys. (Paris)* **1979**, *40*, 99.

(9) Akcasu, A. Z.; Han, C. C. *Macromolecules* **1979**, *12*, 276.
(10) Kuhn, W. *Kolloid-Z.* **1934**, *68*, 2.
(11) Burgers, J. M. "Second Report on Viscosity and Plasticity"; North-Holland Publishing Co.: Amsterdam, 1938; Chapter III.
(12) Oseen, C. V. "Hydrodynamics"; Academic Press: Leipzig, 1927.
(13) Zwanzig, R. *J. Chem. Phys.* **1966**, *45*, 1858.
(14) Ullman, R. *J. Chem. Phys.* **1964**, *40*, 2422.
(15) Flory, P. J. *J. Chem. Phys.* **1949**, *17*, 303.
(16) Edwards, S. F. *Proc. Phys. Soc., London* **1965**, *85*, 613.
(17) LeGuillou, J. C.; Zinn-Justin, J. *Phys. Rev. Lett.* **1977**, *39*, 95.
(18) Fixman, M. *J. Chem. Phys.* **1955**, *23*, 1656.
(19) Peterlin, A. *J. Chem. Phys.* **1955**, *23*, 2464.
(20) Ullman, N.; Ullman, R. *J. Math. Phys.* **1966**, *7*, 1743.
(21) Schlitt, D. W. *J. Math. Phys.* **1968**, *9*, 436.
(22) Davis, P.; Rabinowitz, P. *J. Res. Natl. Bur. Stand.* **1956**, *56*, 35.
(23) Zimm, B. H.; Roe, G. M.; Epstein, L. F. *J. Chem. Phys.* **1956**, *24*, 279.
(24) François, J.; Schwartz, T.; Weill, G. *Macromolecules* **1980**, *13*, 564.
(25) Flory, P. J. "Principles of Polymer Chemistry"; Cornell University Press: Ithaca, N.Y., 1953; Chapter XIV.
(26) Yamakawa, H. "Modern Theory of Polymer Solutions"; Harper and Row: New York, 1971; Chapter VII.
(27) Akcasu, A. Z.; Benmouna, M.; Alkhafaji, S., private communication.
(28) Slagowski, E. L. Doctoral Dissertation, University of Akron, 1972 (available from University Microfilms, Ann Arbor, Mich. 48108).
(29) Altares, T., Jr.; Wyman, D. P.; Allen, V. R. *J. Polym. Sci., Part A* **1964**, *2*, 4533.
(30) Yamaguchi, N.; Sugiuru, Y.; Okano, K.; Wada, E. *J.* Phys. *Chem.* **1971**, *75*, 1141.
(31) Einaga, Y.; Miyaki, Y.; Fujita, H. *J. Polym. Sci., Polym. Phys. Ed.* **1979**, *17*, 2103.
(32) King, T. A.; Know, A.; Lee, W. I.; McAdam, J. D. G. *Polymer* **1973**, *14*, 151.
(33) King, T. A.; Knox, A.; McAdam, J. D. G. *Polymer* **1973**, *14*, 293.
(34) Adam, M.; Delsanti, M. *Macromolecules* **1977**, *10*, 1229.
(35) Yoon, D. Y.; Sundararajan, P. R.; Flory, P. J. *Macromolecules* **1975**, *8*, 776.
(36) Munk, P.; Gutierrez, B. O. *Macromolecules* **1979**, *12*, 467.

Photoresponsive Polymers. 3.[1] Reversible Solution Viscosity Change of Poly(methacrylic acid) Having Spirobenzopyran Pendant Groups in Methanol

Akira Menju, Koichiro Hayashi, and Masahiro Irie*

The Institute of Scientific and Industrial Research, Osaka University, Suita, Osaka 565, Japan. *Received October 24, 1980*

ABSTRACT: Reversible control of solution viscosity by as much as 50% has been achieved upon alternate irradiation with visible ($\lambda > 470$ nm) and ultraviolet (410 nm $> \lambda >$ 310 nm) light, using poly(methacrylic acid) having spirobenzopyran pendant groups in methanol. A large conformational change of the polymer chain was caused by the photoisomerization of the spirobenzopyran attached to the pendant groups. The disappearance/reappearance of the zwitterion structures (merocyanines) on the pendant groups upon visible/ultraviolet light irradiation is considered to alter the balance of the intrachain interactions, resulting in the expansion/contraction of the polymer chain.

Introduction

Although several attempts have been reported to control the conformation of synthetic polymers by photoirradiation, the studies are limited to polymer systems having covalently bound azobenzene residues in the pendant groups[2,4,5] or adsorbed azo dyes[2,3] and the observed effects are very small. Other photoisomerizable chromophores, such as spirobenzopyrans or indigos, are also considered to be useful as well. We have tried to attach spirobenzopyrans to the pendant groups of polymers as chromophores capable of transforming light energy into a change in main-chain conformation.[6]

Spirobenzopyrans are well-known photochromic molecules, which isomerize from the spiropyran to the intensely colored merocyanine form under ultraviolet irradiation; the merocyanines can return thermally or photochemically to the colorless spiropyrans as follows:[7]

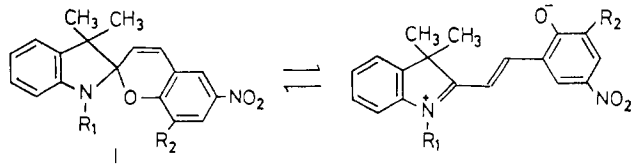

In polar solvents, such as alcohols, colored merocyanines form even in the dark and are in equilibrium with colorless spiropyrans. Photoexcitation of the merocyanines with visible light in alcohols brings about ring closure, with production of colorless spiropyrans; the red color disappears on irradiation with visible light.

In a previous paper,[6] we reported a reversible photodecrease of solution viscosity of poly(methyl methacrylate) having spirobenzopyran pendant groups in nonpolar solvents. The viscosity change was caused by intramolecular solvation by the ester side groups of the photogenerated polar merocyanines. In polar solvents we could not observe any appreciable viscosity decrease by photoirradiation of this polymer.

In this article, we report photoinduced conformational changes observed in poly(methacrylic acid) having spirobenzopyran pendant groups in polar solvents. Methanol solutions of the polymer have a red color, which indicates that merocyanines are formed in the pendant groups in equilibrium with spirobenzopyran in the polar solvent. Visible light irradiation of the solution displaces the equilibrium toward the formation of spirobenzopyran. The disappearance of the merocyanines is expected to alter the equilibrium conformation of the main chain, since the isomerization is associated with a large decrease of the dipole moment of the side chains.

Experimental Section

Polymers having spirobenzopyran pendant groups were synthesized by copolymerization of 1,3,3-trimethylindolino-6′-nitro-8′-[(methacroyloxy)methyl]spirobenzopyran (1, $R_1 = CH_3$; $R_2 = CH_2OCOC(CH_3)=CH_2$) with methacrylic acid by radical initiation.[6] The content of spirobenzopyran in the polymers was

0024-9297/81/2214-0755$01.25/0